Available online at www.sciencedirect.com
SCIENCE DIRECT®
Catalysis Today 99 (2005) 365–373
CATALYSIS TODAY
www.elsevier.com/locate/cattod

Hydrodesulfurization of model diesel using Pt/Al_2O_3 catalysts prepared by supercritical deposition

Shaker Haji[a], Ying Zhang[a], Dafei Kang[b], Mark Aindow[b], Can Erkey[a,*]

[a]*Department of Chemical Engineering, University of Connecticut, Storrs, CT 06269, USA*
[b]*Department of Metallurgy and Materials Engineering, Institute of Materials Science, University of Connecticut, Storrs, CT 06269, USA*

Available online 21 December 2004

Abstract

Pt/Al_2O_3 catalysts with Pt loadings ranging from 0.5 to 11 wt.% were synthesized by supercritical carbon dioxide ($scCO_2$) deposition method. Transmission electron microscopy (TEM) images showed that the synthesized catalysts contained small Pt nanoparticles (1–4 nm in diameter) with a narrow size distribution, no observable agglomeration, and uniformly dispersed on the alumina support. The catalysts were found to be active for hydrodesulfurization of dibenzothiophene (DBT) dissolved in *n*-hexadecane (*n*-HD) without sulfiding the metal phase. The reaction proceeded only via the direct hydrogenolysis route in the temperature range 310–400 °C and at atmospheric pressure. The activity increased with increasing the metal loading. Increasing $[H_2]_0/[DBT]_0$ by either increasing $[H_2]_0$ or decreasing $[DBT]_0$, increased the DBT conversion. At a fixed weight hourly space velocity and feed concentration, conversion did not increase with increasing temperature beyond 330 °C. The presence of toluene inhibited the catalyst activity presumably due to competitive adsorption between DBT and toluene. Under the operating conditions, the reaction was far from equilibrium.

Keywords: Hydrodesulfurization; Supercritical deposition; Diesel; Fuel cell

1. Introduction

Fuel cells are promising alternatives to currently used power generating devices due to their high-energy efficiencies and low environmental emissions. Even though hydrogen is the ideal fuel for various types of fuel cells, lack of a hydrogen distribution infrastructure and challenges in storing it necessitate the development of technologies for extraction of hydrogen from liquid fuels such as methanol, ethanol, natural gas, gasoline and diesel [1]. Among these fuels, diesel is preferred over other fuels such as methanol and natural gas in a wide variety of applications, due to its high-energy density (42.5 MJ/kg for diesel versus 19.9 MJ/kg for methanol, LHV), wide availability and ease of storage.

An important consideration in reforming of petroleum-based fuels, such as gasoline and diesel, is that they contain significant amounts of sulfur-containing compounds such as thiophenes, benzothiophenes and dibenzothiophenes. In the case of diesel, the sulfur-containing compounds are mainly non-substituted and substituted benzothiophenes and dibenzothiophenes [2]. Currently, the sulfur level in diesel is generally around 500 parts per million by weight (ppmw), however, it ranges between 0.5 and 3000 ppmw depending on the fuel source. The presence of such compounds at these concentrations has a detrimental effect on the performance of catalysts used in internal or external reforming and the fuel cell stacks. Therefore, diesel needs to be desulfurized to concentration of less than 0.1 ppmw sulfur before being fed into a fuel cell stack. The technologies that are suitable for desulfurization for fuel cell applications can be broadly classified into two categories:

1. Catalytic transformation (hydrodesulfurization, HDS) [3,7,8].
2. Physico-chemical separation [4,5,6].

HDS has been in use in refineries for the past 50 years to reduce the sulfur content of fossil fuels. The organosulfur compounds are reacted with hydrogen in the presence of a

* Corresponding author.
E-mail address: cerkey@engr.uconn.edu (C. Erkey).

0920-5861/$ – see front matter © 2004 Elsevier B.V. All rights reserved.
doi:10.1016/j.cattod.2004.10.011

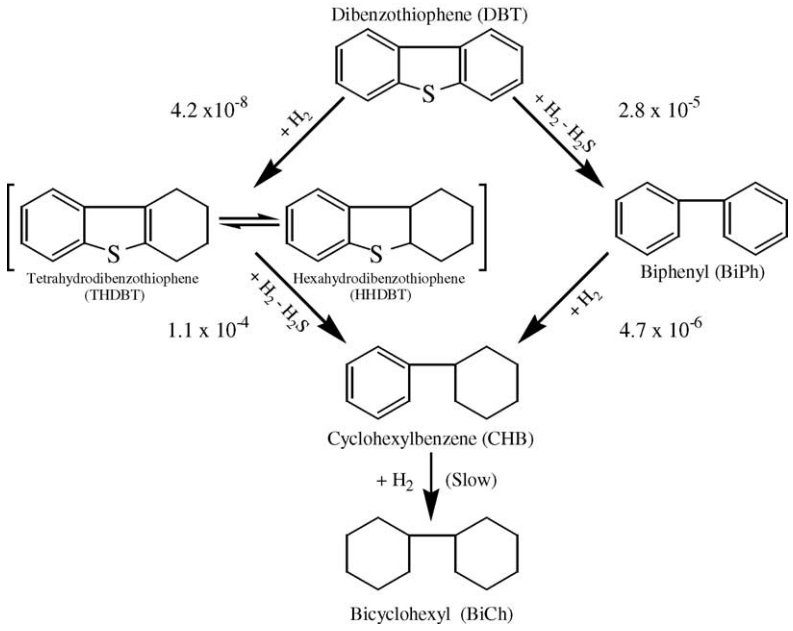

Fig. 1. Proposed reaction network by Houalla et al. [10] for the conversion of DBT and hydrogen in the presence of sulfided $CoMo/Al_2O_3$ at 300 °C and 102 atm. The numbers next to the arrows are the pseudo first-order rate constants ($m^3/(kg\ cat\ s)$).

catalyst, and converted to hydrogen sulfide and sulfur-free organic compound(s). HDS reactors in refineries are currently operated at moderate temperatures (300–360 °C) and at hydrogen pressures of 3.0–5.0 MPa, usually with $CoMo/Al_2O_3$ or $NiMo/Al_2O_3$ catalysts [7,8]. The catalyst is activated by treatment with a mixture of H_2S and H_2 or a feed containing sulfur compounds and H_2 [9].

The exact mechanism of HDS is not known, however, it is generally accepted that HDS proceeds through the reaction network proposed by Houalla et al. [10,11], as shown in Fig. 1 for the HDS of DBT at 300 °C and 102 atm. In the parallel pathway mechanism, the majority of the cyclohexylbenzene (CHB) is produced by the reaction of the reactive intermediate shown in Fig. 1, tetrahydrodibenzothiophene (THDBT) or hexahydrodibenzothiophene (HHDBT). This pathway is also referred to as hydrogenation pathway (HYD) since the sulfur compound is hydrogenated prior to desulfurization. There is a finite contribution to the formation of CHB from the sequential reaction of biphenyl (BiPh) which is formed via direct C–S bond hydrogenolysis of DBT. This pathway is known as hydrogenolysis pathway or direct desulfurization (DDS). In this mechanism, the reaction proceeds via the path of least hydrogen consumption and the hydrogenation of biphenyl and cyclohexylbenzene is slow.

An extensive number of studies have been reported in the literature on synthesis, characterization and activity of catalysts for HDS. Houalla et al. [10] found that the CHB concentration with a $NiMo/Al_2O_3$ catalyst was about three times higher than that with a comparable $CoMo/Al_2O_3$ catalyst. Mochida and co-workers [12] also studied the effect of different metals on the reaction pathways. It was found that $NiMo/Al_2O_3$ exhibited higher HDS activity toward 4,6-DMDBT than $CoMo/Al_2O_3$. This was ascribed to the higher hydrogenation activity of $NiMo/Al_2O_3$ catalyst by comparison of the concentrations of CHB and BiPh in the product mixture. Hydrogenation of the aromatic rings was considered to alleviate the steric hindrance encountered in the HDS of 4,6-DMDBT, which was considered to be the reason for its low reactivity [12]. Mochida and co-workers [13] performed a study using a blend of CoMo and Ru/Al_2O_3 catalysts and compared the activity with those of $CoMo/Al_2O_3$, $NiMo/Al_2O_3$ and Ru/Al_2O_3. The blend showed the highest rate of HDS of 4,6-DMDBT.

Supported platinum was also studied as a catalyst for HDS under standard industrial conditions. Vasudevan and coworkers [14] compared Pt-based catalysts with the commercial $CoMo/Al_2O_3$ in HDS of commercial diesel fuel. It was found that both Pt/HY zeolite and Pt/ASA (amorphous silica-alumina) were more active than the $CoMo/Al_2O_3$ catalyst. Kabe and coworkers [15] also compared unsulfided Pt/Al_2O_3 (3 wt.%), with the conventional $CoMo/Al_2O_3$ catalyst and showed that both had similar activity for HDS of DBT in decalin. Ten percentage of DBT conversion occurred via hydrogenation route with 2 wt.% Pt/Al_2O_3 compared to 7% when conventional CoMo catalyst was used. Considering that hydrogenation followed by desulfurization will be the most likely route to desulfurize hindered dibenzothiophenes [7], van Veen and coworkers [16,17] used catalysts with high-hydrogenation activity to desulfurize 4-ethyl, 6-methyl dibenzothiophene (4E6MDBT). The HDS activity was in the following order: Pt/ASA% $\gg$ Pt/Al_2O_3 > NiW/Al_2O_3 $\gg$ $CoMo/Al_2O_3$ or $NiMo/Al_2O_3$. The superiority of Pt/ASA in HDS of 4E6MDBT was attributed to its superior hydrogenation activity. It was also reported that both sulfided and unsulfided Pt/ASA had similar catalytic activities.

The catalyst preparation method also had an effect on the HDS activity. Venezia et al. [18] studied the influence of the preparation method of CoMo/silica catalysts on the thiophene HDS activity. The catalysts were prepared by either total sol–gel route or incipient wetness impregnation/co-impregnation and the results were compared with catalysts supported on commercial silica. The catalyst supported on sol–gel silica with the two metals loaded by co-impregnation in the presence of nitrilotriacetic acid showed the highest activity. Kordulis and coworkers [19] found that in case of $CoMo/Al_2O_3$, the catalyst prepared by depositing first the Mo precursor through equilibrium deposition filtration (EDF) and then Co precursor via dry impregnation resulted in catalysts that had higher activity than the catalysts prepared by co-EDF or by a conventional impregnation technique.

Recently, we reported on the synthesis of carbon aerogel supported platinum using a supercritical deposition method with good control of average platinum particle size [20]. In this method, dimethyl(1,5-cyclooctadiene)platinum(II) ($CODPtMe_2$) was dissolved in supercritical CO_2 ($scCO_2$) and impregnated into porous organic and carbon aerogels. The impregnated aerogels were converted to carbon aerogel supported platinum by heat treatment ranging from 300 to 1000 °C in the presence of nitrogen gas. Both conventional and high-resolution transmission electron microscopy (TEM) micrographs showed a good distribution of fairly monodisperse Pt particles throughout the bulk of all the aerogel supports used. Particle sizes obtained from H_2 and CO chemisorption measurements were consistent with those measured from TEM images, indicating the accessibility of the surface of platinum crystallites. In this article, we report the results of our studies on HDS of DBT in hexadecane using Pt/Al_2O_3 catalysts prepared by supercritical deposition.

2. Experimental

2.1. Preparation of catalyst

The experimental set-up used in the preparation of the Pt/Al_2O_3 catalyst is shown in Fig. 2. Desired amount of organometallic precursor dimethyl(1,5-cyclooctadiene)platinum(II), 99% Strem, stirring bar and the support (γ-Alumina, Saint-Gobain-Norpro, SA 6175 1/8″ pellets, 260 m^2/g) were placed into a high-pressure vessel. The support was heated in air for 2 h at 300 °C before it was placed in the vessel to remove any adsorbed moisture. The vessel was sealed and then heated to 80 °C. Subsequently, it was charged slowly with CO_2 using a syringe pump (ISCO 260D) up to the pressure of 27.6 MPa and kept at these conditions for 24 h. Then, the vessel was depressurized through a restrictor into the atmosphere. After the vessel was cooled down, the precursor/support composite was taken out. The actual adsorbed amount of the precursor was determined by the weight change of the support using an analytical balance (Adventure Model AR2140) accurate to ±0.1 mg. The metal loading amount was calculated from the adsorbed precursor amount during the impregnation step.

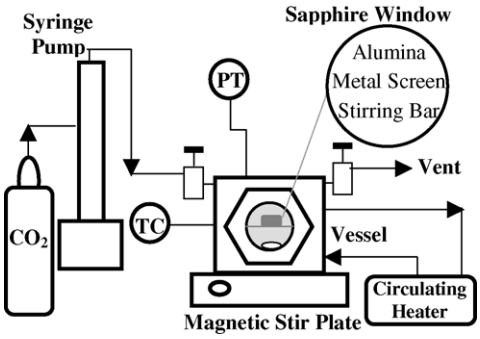

Fig. 2. The experimental set-up used for supercritical carbon dioxide deposition.

The precursor/support composite obtained as explained above was placed in a tube that was placed into a tube furnace (Thermolyne 21100) for thermal reduction of the organometallic precursor. The deposited precursor was reduced thermally at 300 °C in the presence of nitrogen gas with a flow rate of 100 cm^3/min. The choice of the reduction temperature was based on TGA of the precursor [20]. The thermal decomposition was continued for 6 h. The commercial 0.52 wt.% Pt/Al_2O_3 was purchased from Aldrich.

2.2. Transmission electron microscopy

Specimens for TEM examination were prepared by carefully crushing the metal/support samples with a mortar and pestle set. The resulting powders were suspended in a volatile solvent, and ultrasonicated to obtain a uniform suspension. One or two drops of this suspension were deposited onto a copper mesh grid coated with a holey carbon film. The TEM specimens were then allowed to dry completely before examination in a JEOL 2010 FasTEM operating at 200 kV. This instrument is equipped with a high-resolution objective lens pole-piece (spherical aberration coefficient $C_s = 0.5$ mm) giving a point-to-point resolution of <0.19 nm in phase contrast images.

2.3. HDS reactions with model diesel

The evaluation of catalytic activity was carried out in a fixed-bed reactor. The reactor consisted of two pieces of 0.18″i.d. × 1/4″o.d. × 8.5″L 316 stainless-steel tubing connected together with a Union Tee. A type K thermocouple was inserted in the third bore of the tee. The tubing was treated with Sulfinert® (Restek) to prevent corrosion due to the sulfur present in the fuel. The reactor was packed with 0.92 g catalyst (particle size: 0.50–0.125 mm) and plugged in both sides with quartz wool. The reactor was placed in the middle of a tubular furnace (Thermolyne

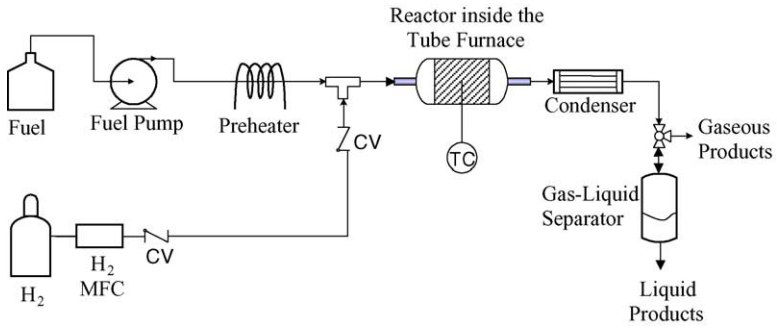

Fig. 3. The experimental set-up for the hydrodesulfurization (HDS) process.

21,100) as shown in Fig. 3. Hydrogen (Airgas, ultra high purity)) was delivered to the reactor using mass flow controllers (Celerity Model 7301) while the liquid fuel was fed with a HPLC pump (Isco Model 2350). The liquid was vaporized before it was introduced along with the hydrogen to the reactor. For each run, hydrogen was first passed over the catalyst bed at a flow rate of 100 N ml/min and 400 °C. Subsequently, the reactor was cooled to the desired temperature under flowing hydrogen. Once the desired temperature was reached, the hydrogen flow rate was adjusted and the liquid fuel was fed to the reactor. The fuel consisted of DBT (Aldrich, >99%) dissolved in *n*-hexadecane (ICN, >99%) or a mixture of the latter with toluene (Aldrich, >99.5%). The DBT concentration in the fuel was 250 ppmw S, unless otherwise was mentioned. The effluent from the reactor was passed through a condenser and collected in a gas–liquid separator. The gas stream was analyzed for H_2S using a gas chromatograph (HP 6890) equipped with a sulfur-specific flame photometric detector (S-FPD) and a capillary column (J&W Scientific HP-5). The liquid stream was analyzed for DBT using a gas chromatograph (HP 6890) equipped with S-FPD and FID detectors and a capillary column (J&W Scientific HP-5). The liquid product was also occasionally analyzed with GC–MS (HP 6890-5892), equipped with a 100% methyl silicon capillary column, to identify the products. In all the runs, a steady state was reached in 1.5–3.5 h depending on the weight hourly space velocity (WHSV) and the steady-state DBT conversion was calculated from the amount of DBT in the feed and the effluent. Octane (Aldrich, anhydrous >99%) was used as an external standard for measuring the compounds' concentrations. The conditions employed in this study are summarized in Table 1. The pseudo first order rate constants (k_{DBT} = m^3/(kg cat s)) reported here were calculated from the following equation:

$$k_{DBT} = \frac{-F_{T0}RT}{WP}\ln(1-X)$$

where F_{T0} is the feed molar flow rate (*n*-HD + H_2), R the universal gas constant, T the reaction temperature, W the catalysts weight, and X the conversion. The equilibrium conversion of certain reactions in a flow reactor were calculated using Aspen Plus (Version 12.1) from Aspen Technology Inc.

Table 1
Experimental conditions

$[DBT]_0$ (ppmw S)	111–887
Feed	*n*-HD or *n*-HD + toluene
Pressure (atm)	1
Temperature (°C)	310–400
H_2 flow rate (N ml/min, 25 °C and 1 atm)	5.1–66.4
Fuel flow rate (ml/min, 25 °C and 1 atm)	0.088–0.55
H_2/(*n*-HD) molar ratio (or volume ratio, Nl/l)	0.28–3.63 (or 23.3–301.8)
Platinum loading (wt.%)	0.5–11.0
WHSV (h^{-1})	4.47–27.92

3. Results and discussion

TEM was used to characterize the synthesized and commercial Pt/Al_2O_3 catalysts. Phase-contrast TEM images obtained from the samples revealed clearly the morphology of the alumina supports, and in the thinnest regions the Pt nanoparticles could also be resolved. In thicker regions of the support, a combination of projection effects and increased inelastic scattering obscured the contrast from these particles. Nonetheless, by careful selection of the image regions for analysis, measurements of particle sizes and distributions were obtained. Fig. 4 is a high-resolution TEM micrograph obtained from a sample of commercial 0.52 wt.% Pt/Al_2O_3 showing a group of Pt nanoparticles dispersed on the alumina support. We note that due to the very low loading, it is difficult to observe the Pt nanoparticles in most areas. These particles were, however, distributed inhomogeneously and thus Fig. 4 is not typical of the overall distribution but instead represents an area with an unusually high-nanoparticle density.

A representative high-resolution TEM image which reveals the plate-like morphology of the pure alumina support used in this study is shown in Fig. 5(a). Fig. 5(b)–(e) are corresponding images obtained from the catalysts prepared in our laboratory using the $scCO_2$ deposition method. These materials were found to contain small Pt nanoparticles (<4 nm in diameter) with a narrow size

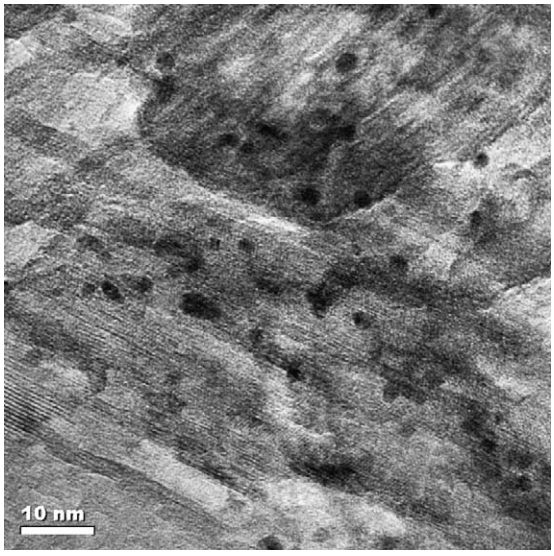

Fig. 4. TEM micrograph of the commercial 0.52 wt.% Pt/Al_2O_3 showing a group of Pt nanoparticles dispersed on the alumina support.

distribution, no observable agglomeration, and uniformly dispersed on the alumina support. As such, the images are typical of these materials and no examples of large particles were observed in these samples. There is a small but measurable increase in the average particle size with increasing metal loading and the approximate particle size range for each of the catalysts is as follows: 0.58% Pt (1.0–1.5 nm), 1.26% Pt (1.5–2.5 nm), 5.7% Pt (1.8–2.7 nm), and 11% Pt (2.0–3.6 nm).

Preliminary runs were carried out at various conditions and the product streams were analyzed. The gas product stream was analyzed with GC (S-FPD) for H_2S concentration to obtain sulfur mole balance closure. The difference between the measured H_2S concentration and the calculated (from DBT conversion) ranged from −16 to +18%. The liquid stream was analyzed with GC (S-FPD, FID) and GC–MS for identification of reaction products. Besides DBT and *n*-HD, traces of organic compounds (C_5–C_{13}, 10–100 ppmw each) were detected indicating that *n*-hexadecane was cracking catalytically in the presence of hydrogen. The compounds were mainly saturated alkanes; however, at a very low H_2/(*n*-HD) molar ratio (0.08) and a high temperature (400 °C), both alkanes and alkenes were detected. Interestingly, among the possible products of HDS of DBT (i.e. BiPh, CHB, DCH), only BiPh was detected which indicates that at atmospheric pressure HDS of DBT proceeds only via hydrogenolysis route (DDS), as opposed to both DDS and HYD routes at high pressure. Such an observation was also reported by Bartsch and Tanielian [21] with $CoMo/Al_2O_3$ catalysts where the products were merely H_2S and BiPh at atmospheric pressure. The hydrogenation of DBT followed by desulfurization is limited thermodynamically at atmospheric pressure and high temperature. The calculated equilibrium conversion of DBT to BiPh was found to be 99.60%, while that of DBT to CHB was 0.40%. The conditions under which the equilibrium concentrations were calculated were same as those given in Fig. 6 (T = 310 °C, P = 1 atm, $y_{(H_2)_0}$ = 0.71, $y_{n\text{-HD}_0}$ = 0.29, y_{DBT_0} = 8.87E-5, and *n*-HD was assumed to be inert). On the other hand, at high pressures, for example 40 atm, the equilibrium conversions were 0.20% for the reaction of DBT to BiPh and 99.80% for the conversion of DBT to CHB.

The stability of commercial Pt/Al_2O_3 was studied for HDS reaction at low H_2/fuel ratios and atmospheric pressure. The catalyst was found to be stable for 14 h as shown in Fig. 6. To study the period before the reactor reached steady state, the run was carried out at a low space velocity. As shown in Fig. 7, in the first hour, 80% of DBT was removed due to reaction with hydrogen to produce BiPh, while the remaining 20% was removed by adsorption on the support. After an hour, the active adsorption sites in the support were almost saturated and the DBT concentration started to increase in the effluent while the DBT removal was dominated by chemical conversion to BiPh. In around 2 h, DBT was only removed by chemical reaction and the amount removed from solution stopped decreasing as the catalyst activity stopped decreasing.

The catalytic activity of the synthesized Pt/Al_2O_3 catalysts along with the commercial one were compared at different hydrogen/(*n*-hexadecane) molar ratios in the feed as shown in Fig. 8. As the metal loading increased, the catalytic activity increased. Similar result was reported by Kabe et al. [22] when 2, 4, and 6 wt.% Pt/Al_2O_3 was studied in HDS of DBT under high pressure conditions. This is expected since the total surface area of the metal would increase as the metal loading increases given that the particles do not agglomerate significantly which is the case with the three synthesized catalysts as shown by TEM images. The values of pseudo first order rate constants (m^3/(kg cat s)) were: 0.58% Pt (9.2×10^{-4}), 1.26% Pt (1.71×10^{-3}), and for 5.7% Pt (3.3×10^{-3}) at H_2/(*n*-HD) of 1.25 molar ratio. It was also found that the commercial and the in-house prepared catalysts with similar loadings have similar catalytic activities.

The effect of $[H_2]_0/[DBT]_0$ on conversion of DBT was also studied. As shown in Fig. 9, at a fixed hydrogen and fuel flow rate, the DBT conversion increased as the DBT concentration in the feed solution decreased, showing that the HDS of DBT is not exactly first order in DBT concentration as assumed in many studies. The DBT conversion increased as the $[H_2]_0/[DBT]_0$ increased at all DBT feed concentrations and hydrogen flow rates employed.

The effect of reaction temperature on the catalyst activity was found to be interesting. As shown in Fig. 10, the DBT conversion increased substantially as the temperature was increased from 310 to 330 °C. However, further increases in temperature barely had any effect on the conversion. Such behavior can perhaps be attributed to formation of species that inhibit the HDS reaction, such as coke or other organic compounds. The same behavior was recorded by Gates and

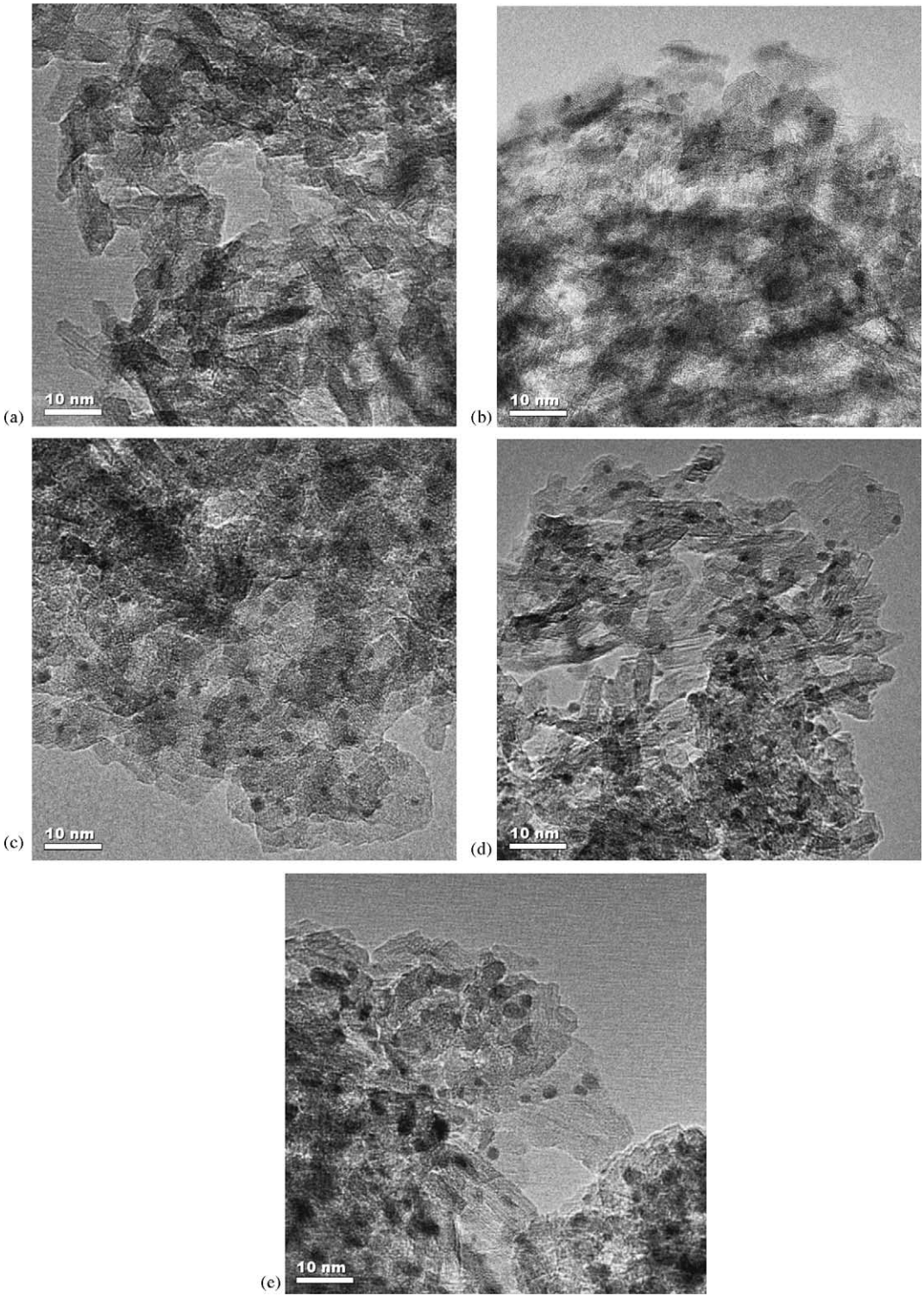

Fig. 5. High-resolution TEM micrograph showing (a) the basic morphology of the alumina support used in this study and images of the Pt/Al_2O_3 at different metal loadings, (b) 0.58 wt.% Pt, (c) 1.26 wt.% Pt, (d) 5.7 wt.% Pt, and (e) 11 wt.% Pt.

coworkers [23] for $CoMo/Al_2O_3$ catalyst under atmospheric pressure. In our experiments, product color changed gradually from clear at 310 °C to yellowish as the temperature was increased (Fig. 10). The change in the color with the increase of hydrotreating temperature was also reported in other studies [8].

Besides paraffins, commercial diesel contains 5.5–84% aromatics depending on the constituent blends [5,8,24]. Jongpatiwut et al. reported that, at 300 °C and 35 atm, the presence of sulfur (DBT) inhibited the hydrogenation of naphthalene and phenanthrene over $Pt–Pd/Al_2O_3$ in model diesel where DBT was hydrodesulfurized [25]. Similar

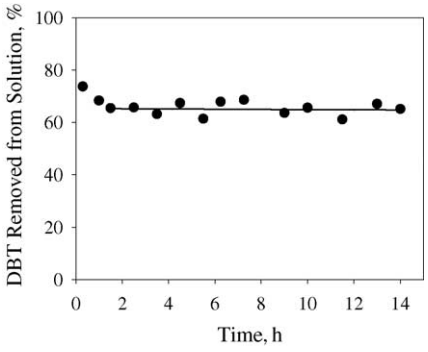

Fig. 6. Dependence of DBT conversion on time on-stream. Reaction conditions: $P = 1$ atm, $T = 310$ °C, n-HD flow rate = 0.22 ml/min, $H_2/(n\text{-HD}) = 2.46$ molar ratio, WHSV = 11.3 h^{-1}, and 0.52 wt.% Pt/Al_2O_3 commercial.

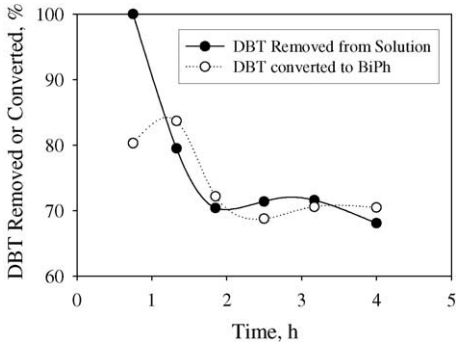

Fig. 7. Initial DBT removal by both adsorption on support and chemical reaction. Reaction conditions: $P = 1$ atm, $T = 310$ °C, n-HD flow rate = 0.088 ml/min, $H_2/(n\text{-HD}) = 1.24$ molar ratio, WHSV = 4.5 h^{-1}, and 0.58 wt.% Pt/Al_2O_3.

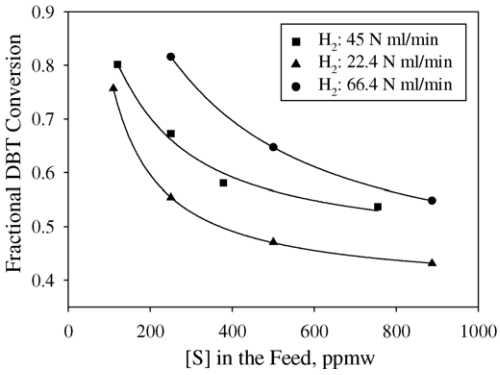

Fig. 9. The effect of $[H_2]_0/[DBT]_0$ on DBT conversion. Reaction conditions: $P = 1$ atm, $T = 310$ °C, n-HD flow rate = 0.22 ml/min, and 0.52 wt.% Pt/Al_2O_3.

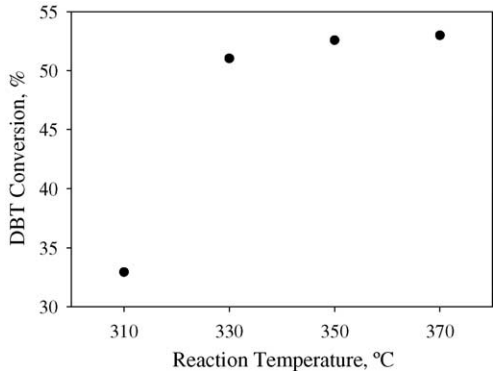

Fig. 10. The effect of temperature on DBT conversion. Reaction conditions: $P = 1$ atm, n-HD flow rate = 0.22 ml/min, $H_2/(n\text{-HD}) = 0.5$ molar ratio, WHSV = 11.1 h^{-1}, and 0.58 wt.% Pt/Al_2O_3.

results where obtained by van Veen and coworkers [17] when the hydrogenation of BiPh over Pt/Al_2O_3 was studied in the presence of 4E6MDBT. Because of the two reasons mentioned above, the presence of aromatics in real diesel and the reported effect of organosulfur compounds on hydrotreatment of aromatics, the HDS of DBT was examined in the presence of an aromatic. Reactions were carried out using a solution of 10 wt.% toluene in n-hexadecane that contained 250 ppmw S DBT and the result was compared to DBT in n-HD solution. As shown in Fig. 11, the presence of toluene inhibited the hydrodesulfurization of DBT and the inhibition was more pronounced at low H_2/fuel ratios. When the liquid product of HDS of DBT in n-HD plus toluene solution was analyzed using GC–MS,

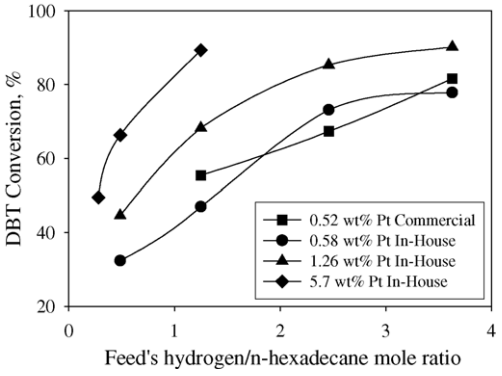

Fig. 8. Catalysts' activity comparison. Reaction conditions: $P = 1$ atm, $T = 310$ °C, and n-HD flow rate = 0.22 ml/min.

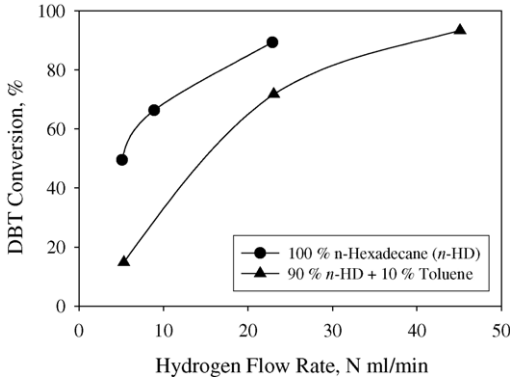

Fig. 11. Solvent's effect on DBT conversion. Reaction conditions: $T = 310$ °C, fuel flow rate = 0.22 ml/min, and 5.7 wt.% Pt/Al_2O_3.

the product of toluene hydrogenation, methylcyclohexane (MCH), could not be detected. However, it is known that the hydrogenation of toluene is retarded at elevated temperatures [26] and that the hydrogenation of aromatics in general is limited thermodynamically at atmospheric pressure and high temperatures. For instance, at the given experimental condition, where H_2 flow is 23.1 N ml/min and assuming that *n*-HD is inert, the calculated equilibrium conversion of the hydrogenation of toluene to MCH was found to be only 0.61%, which is very low if compared to that at higher pressures (e.g. 98.28% at 35 atm). In spite of the thermodynamic limitation of the hydrogenation of toluene at the operating temperature and pressure, a slight conversion (as low as 0.001%) of toluene to MCH could be detected due to the high concentration of the former in the feed. When the above solution (10 wt.% toluene in *n*-hexadecane) was hydrogenated under the same conditions but without the presence of DBT in solution, MCH was detected in the product stream at ~33 ppmw indicating a toluene conversion of 0.03%. By comparing the two experiments, it was concluded that while toluene suppressed the hydrogenolysis of DBT, it was not hydrogenated. This suggests that the inhibition is not due to hydrogen consumption for toluene hydrogenation, but it is merely due to competition for active sites. These findings differ from the results of van Veen and coworkers [17] where it was shown that the desulfurization of 4E6MDBT was rather unaffected by the presence of biphenyl but the hydrogenation of biphenyl was strongly retarded. However, this could be due to the difference in the reaction conditions, namely the very low BiPh concentration (100 ppm) in solution and the high H_2/fuel ratio employed in their study. Interestingly, Prins and coworker [27] reported that the use of toluene as a solvent had no effect on the HDS of DBT and 4,6-DMDBT at 340 °C and 5 MPa, however, traces of naphthalene had an inhibitive effect.

As the residence time increased, conversion of DBT increased as shown in Fig. 12 indicating that the reaction is far from equilibrium.

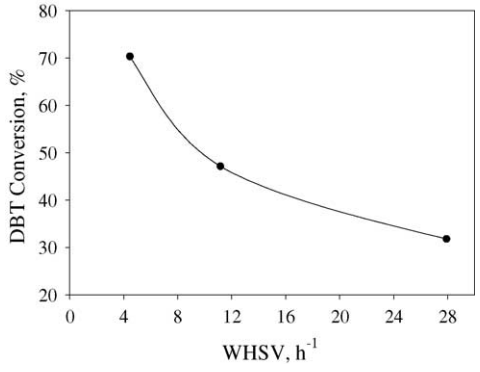

Fig. 12. The effect of WHSV on DBT conversion. Reaction conditions: $P = 1$ atm, $T = 310$ °C, H_2/(*n*-HD) = 1.23 molar ratio, and 0.58 wt.% Pt/Al_2O_3.

4. Conclusion

Hydrodesulfurization of DBT dissolved in *n*-hexadecane was studied over unsulfided Pt/Al_2O_3 catalysts at atmospheric pressure. The studies were carried out using commercial catalysts and also catalysts that were prepared by supercritical carbon dioxide deposition method. TEM images showed that the catalysts prepared via the supercritical route contained small Pt nanoparticles (<4 nm in diameter) with a narrow size distribution, no observable agglomeration, and uniformly dispersed on the alumina support. The catalysts were stable and DBT concentration in the feed could be reduced to less than 0.1 ppmw at sufficiently high $[H_2]_0/[DBT]_0$ and low WHSV (for example, 1.2 g 0.52 wt.% Pt/Al_2O_3, $T = 360$ °C, $P = 1$ atm, WHSV = 4.9 h^{-1}, H_2/(*n*-HD) molar ratio = 7.3, and $[DBT]_0 = 250$). The initial decrease in DBT removal was found not to be solely due to catalyst initial deactivation, but also due to the breakthrough of DBT adsorbed on the support. The activity increased with increasing metal loading. Increasing $[H_2]_0/[DBT]_0$ increased the DBT conversion and increasing temperature increased the conversion until 330 °C. The presence of toluene inhibited the catalyst activity due to competitive adsorption between DBT and toluene and conversion increased with increasing residence time.

Acknowledgement

This research was supported by the US Army CECOM (OT DAAB07-03-3-K415). The authors would like to thank Saint-Gobain NorPro Corporation for providing the alumina support and Mr. Gary Lavigne for analysis of the samples with GC–MS.

References

[1] S. Thomas, M. Zalbowitz, Fuel Cells-Green Power, Los Alamos National Laboratory, 1999.
[2] C. Song, X. Ma, Appl. Catal. B 41 (2003) 207.
[3] J. Larminie, A. Dicks, Fuel Cell Systems Explained, John Wiley & Sons, England, 2002.
[4] X. Ma, L. Sun, C. Song, Catal. Today 77 (2002) 107.
[5] A.J. Hernandez-Maldonado, R.T. Yang, Ind. Eng. Chem. Res. 42 (2003) 123.
[6] S. Haji, C. Erkey, Ind. Eng. Chem. Res. 42 (2003) 6933.
[7] R. Shafi, G.J. Hutchings, Catal. Today 59 (2000) 423.
[8] D.D. Whitehurst, I. Isoda, I. Mochida, Adv. Catal. 42 (1998) 345.
[9] C.N. Saterfield, Hetrogeneous Catalysis in Industrial Practice, second ed. McGraw-Hill, New York, 1993.
[10] M. Houalla, N.K. Nag, A.V. Sapre, D.H. Broderick, B.C. Gates, AIChE J. 24 (1978) 1015.
[11] M. Houalla, D.H. Broderick, A.V. Sapre, N.K. Nag, V.H.J.D. Beer, J. Catal. 61 (1980) 523.
[12] X. Ma, K. Sakanishi, T. Isoda, I. Mochida, Hydrotreating Technology for Pollution Control, Marcel Dekker, New York, 1996.

[13] T. Isoda, S. Nagao, X.L. Ma, Y. Korai, I. Mochida, Energy Fuels 10 (1996) 482.
[14] R. Navarro, B. Pawelec, J.L.G. Fierro, P.T. Vasudevan, J.F. Cambra, P.L. Arias, Appl. Catal. A 137 (1996) 269.
[15] W. Qian, Y. Yoda, Y. Hirai, A. Ishihara, T. Kabe, Appl. Catal. A 184 (1991) 81.
[16] W.R.A.M. Robinson, J.A.R. van Veen, V.H.J. de Beer, R.A. van Santen, Fuel Processing Technol. 61 (1991) 89.
[17] W.R.A.M. Robinson, J.A.R. van Veen, V.H.J. de Beer, R.A. van Santen, Fuel Processing Technol. 61 (1991) 103.
[18] A.M. Venezia, V.L. Parola, G. Deganello, D. Cauzzi, G. Leonardi, G. Predieri, Appl. Catal. 229 (2002) 261.
[19] Ch. Papadopoulou, J. Vakros, H.K. Matralis, Ch. Kordulis, A. Lycourghiotis, J. Colloid Interface Sci. 261 (2003) 146.
[20] C. Saquing, T.T. Cheng, M. Aindow, C. Erkey, J. Phys. Chem. B. 108 (2004) 7716.
[21] R. Bartsch, C. Taniellian, J. Catal. 35 (1974) 353.
[22] T. Kabe, W. Qian, Y. Hirari, L. Li, A. Ishihara, J. Catal. 190 (2000) 191.
[23] D.R. Kilanowski, H. Teeuwen, V.H.J. de Beer, B.C. Gates, G.C.A. Schuit, H. Kwart, J. Catal. 55 (1978) 129.
[24] H. Yang, Z. Ring, Y. Briker, N. McLean, W. Friesen, C. Fairbridge, Fuel 81 (2002) 65.
[25] S. Jongpatiwut, Z. Li, D.E. Resasco, W.E. Alvarez, E.L. Sughrue, G.W. Dodwell, Appl. Catal. A 262 (2004) 241.
[26] J.L. Rousset, L. Stievano, F.J. Cadete Santos Aires, C. Geantet, A.J. Renouprez, M. Pellarin, J. Catal. 197 (2001) 335.
[27] M. Egorova, R. Prins, J. Catal. 224 (2004) 278.